Ab initio calculations on SCl_2 and low-lying cationic states of SCl_2^+: Franck-Condon simulation of the UV photoelectron spectrum of SCl_2

Daniel K. W. Mok,[a),b)] Foo-tim Chau,[a),c)] and Edmond P. F. Lee[d)]
Department of Applied Biology and Chemical Technology, Hong Kong Polytechnic University, Hung Hom, Hong Kong

John M. Dyke
School of Chemistry, University of Southampton, Highfield, Southampton SO17 1BJ, United Kingdom

(Received 9 March 2006; accepted 13 April 2006; published online 8 September 2006)

Geometry optimization calculations were carried out on the $\tilde{X}\,^1A_1$ state of SCl_2 and the $\tilde{X}\,^2B_1$, $\tilde{A}\,^2B_2$, $\tilde{B}\,^2A_1$, $\tilde{C}\,^2A_1$, $\tilde{D}\,^2A_2$, and $\tilde{E}\,^2B_2$ states of SCl_2^+ at the restricted-spin coupled-cluster single-double plus perturbative triple excitation [RCCSD(T)] level with basis sets of up to the augmented correlation-consistent polarized quintuple-zeta [aug-cc-pV(5+d)Z] quality. Effects of core electron correlation, basis set extension to the complete basis set limit, and relativistic contributions on computed minimum-energy geometrical parameters and/or relative electronic energies were also investigated. RCCSD(T) potential energy functions (PEFs) were calculated for the $\tilde{X}\,^1A_1$ state of SCl_2 and the low-lying states of SCl_2^+ listed above employing the aug-cc-pV(5+*d*)Z basis set. Anharmonic vibrational wave functions of these neutral and cationic states of SCl_2, and Franck-Condon (FC) factors of the lowest four one-electron allowed neutral photoionizations were computed employing the RCCSD(T)/aug-cc-pV(5+d)Z PEFs. Calculated FC factors with allowance for the Duschinsky rotation and anharmonicity were used to simulate the first four photoelectron (PE) bands of SCl_2. The agreement between simulated and observed He I PE spectra reported by Colton *et al.* [J. Electron Spectrosc. Relat. Phenom. **3**, 345 (1974)] and Solouki *et al.* [Chem. Phys. Lett. **26**, 20 (1974)] is excellent. However, our FC spectral simulations indicate that the first observed vibrational component in the first PE band of SCl_2 is a "hot" band arising from the $SCl_2^+\tilde{X}\,^2B_1(0,0,0) \leftarrow SCl_2\tilde{X}\,^1A_1(1,0,0)$ ionization. Consequently, the experimental adiabatic ionization energy of SCl_2 is revised to 9.55 ± 0.01 eV, in excellent agreement with results obtained from state-of-the-art *ab initio* calculations in this work. © *2006 American Institute of Physics*. [DOI: 10.1063/1.2202734]

I. INTRODUCTION

Recently we have published state-of-the-art *ab initio* calculations on the $\tilde{X}\,^1A_1$ state of SF_2 and the $\tilde{X}\,^2B_1$, $\tilde{A}\,^2A_1$, $\tilde{B}\,^2B_2$, $\tilde{C}\,^2B_2$, $\tilde{D}\,^2A_1$, and $\tilde{E}\,^2A_2$ states of SF_2^+.[1] In this study,[1] the Franck-Condon (FC) spectral simulations of the photoelectron (PE) bands, arising from ionizations from the $\tilde{X}\,^1A_1$ state of SF_2 to the one-electron allowed $\tilde{X}\,^2B_1$, $\tilde{C}\,^2B_2$, $\tilde{D}\,^2A_1$, and $\tilde{E}\,^2A_2$ states of SF_2^+, were also presented, and compared with the only available experimental He I PE spectrum of SF_2.[2] As a continuation of our ongoing research program of combined *ab initio*/FC studies on electronic spectra of small molecules,[3–7] we report in the present article a similar computational investigation on the related He I PE spectrum of SCl_2. Two experimental studies[8,9] on the He I PE spectrum of SCl_2 were published in 1974. Similar to the available experimental He I PE spectrum of SF_2,[2] the first PE band of SCl_2 was observed with resolved vibrational structure.[8,9] The vertical ionization energy (VIE) of the first PE band of SCl_2 arising from the ionization from the $\tilde{X}\,^1A_1$ state of SCl_2 to the $\tilde{X}\,^2B_1$ state of SCl_2^+ was measured to be 9.70 and 9.67 eV by Colton and Rabalais,[8] and Solouki *et al.*[9] respectively. [Note that the two He I studies[8,9] have employed different symmetry axis systems for the SCl_2 molecule and hence the b_1 and b_2 irreducible representations are swapped. Here, for the sake of consistency, we have used the axis system of Solouki *et al.*[9] throughout, and the ground state of SCl_2^+ is then the $\tilde{X}\,^2B_1$ state (not the $\tilde{X}\,^2B_2$ state as used by Colton and Rabalais)]. These VIE values correspond to the positions of the fourth vibrational component of the first PE band observed in the two He I PE studies.[8,9] In addition, the adiabatic ionization energy (AIE) of SCl_2 was given to be 9.49 eV by Colton and Rabalais[8] and it corresponds to the position of the first identifiable vibrational component of the first PE band. Although Solouki *et al.*[9] did not give the AIE value of SCl_2 explicitly in their work, it can be evaluated to be 9.45 eV, using the reported vibrational spacing of 530 ± 30 cm^{-1} and assuming that the first observable vibrational component corresponds to the $SCl_2^+\tilde{X}\,^2B_1(0,0,0) \leftarrow SCl_2\tilde{X}\,^1A_1(0,0,0)$ ionization. These AIE values of SCl_2 obtained from He I PE

[a)]Authors to whom correspondence should be addressed.
[b)]Electronic mail: bcdaniel@polyu.edu.hk
[c)]Electronic mail: bcf.tchau@polyu.edu.hk
[d)]Also at University of Southampton. Electronic mail: epl@soton.ae.uk

TABLE I. The ranges of bond length [r(SCl) in angstrom] and bond angle [θ(ClSCl) in degree], and the number of points employed in the RCCSD(T)/aug-cc-pV(5+d)Z energy scans, which were used for the fitting of the potential energy functions (PEFs) of the different electronic states of SCl_2 and its cation, and the maximum vibrational quantum numbers of the symmetric stretching (v_1) and bending (v_2) modes of the harmonic basis used in the variational calculations of the anharmonic vibrational wave functions of each electronic state and the restrictions of the maximum values of (v_1+v_2); see text.

States	Range of r(SCl)	Range of θ(ClSCl)	Points	Max. v_1	Max. v_2	Max. (v_1+v_2)
$\tilde{X}\,^1A_1$	1.30–2.80	61–145	123	10	15	15
$\tilde{X}\,^2B_1$	1.20–2.80	65–149	122	15	20	20
$\tilde{A}\,^2A_1$	1.16–2.45	65–160	120	10	25	25
$\tilde{B}\,^2B_2$	1.27–2.70	37–130	109	25	40	40
$\tilde{C}\,^2A_1$	1.48–2.22	107–174	88	4	8	8
$\tilde{D}\,^2A_2$	1.27–2.70	44–148	123	12	20	20
$\tilde{E}\,^2B_2$	1.45–2.40	70–134	103	5	10	10

studies[8,9] agree very well with an AIE value of 9.45±0.03 eV derived from a later photoionization mass-spectrometry study.[10] However, in the present investigation, it will be shown that the first vibrational component observed in the first PE band of SCl_2 is actually a "hot" band, arising from the $SCl_2^+\tilde{X}\,^2B_1(0,0,0) \leftarrow SCl_2\tilde{X}\,^1A_1(1,0,0)$ ionization and hence, previously reported AIE values of SCl_2 have to be revised based on the present combined *ab initio*/FC study.

In contrast to the observed higher ionization energy (IE) bands of SF_2 in the He I PE spectrum,[2] which are masked heavily by overlapping PE bands of other species, the higher IE bands of SCl_2 reported in both Refs. 8 and 9 have almost no overlapping bands from other species. This is because SCl_2 is the most stable member in the sulphur dihalide series and can be prepared in pure form in the gas phase. However, no resolvable vibrational structure associated with any higher IE bands of SCl_2 was observed in both He I PE studies.[8,9] Nevertheless, Colton and Rabalais[8] employed CNDO/2 and the Mulliken-Wolfsberg-Helmholtz (MWH) calculations, and Solouki *et al.*[9] employed Koopmans' theorem applied to HF/[7*s*4*p*1*d*] calculations, to assign the higher IE bands observed in their He I PE spectra. However, some of their assignments do not agree. Specifically, based on computed VIEs, Colton and Rabalais have assigned the $(b_2)^{-1}$ ionization leading to a $^2B_2$ cationic state to the second band of the He I PE spectrum of SCl_2, and the $(a_1)^{-1}$ and $(a_2)^{-1}$ ionizations, leading to the $^2A_1$ and $^2A_2$ cationic states, respectively, both to the third PE band (see Table I of Ref. 8). However, Solouki *et al.* have assigned the $(a_1)^{-1}$ and $(b_2)^{-1}$ ionizations both to the second PE band, and the $(a_2)^{-1}$ ionization to the third PE band (see Table I of Ref. 9). In addition, some assignments given in the two He I PE studies[8,9] for the even higher IE bands are also different. Nevertheless, it has been pointed out in Ref. 9 that contributions from electron correlation and relaxation need not be the same for different electronic states, and hence the order of the computed VIEs based on Koopmans' theorem may change, if the contributions from electron correlation and relaxation are included in the evaluation of VIEs. In view of tremendous advances in computational quantum chemistry during the last few decades, the calculations carried out over 30 years ago in the two He I PE studies[8,9] have to be considered as relatively low-level by today's standards. In addition, the true VIE position of a PE band depends on the FC factors between the two electronic states involved. In view of the above considerations, the assignments of the higher IE bands in the He I PE spectrum of SCl_2 given in Refs. 8 and 9 based on relatively low level calculations have to be considered as tentative. In the present study, we have carried out state-of-the-art *ab initio* calculations on the low-lying cationic states of SCl_2^+ and also FC calculations including anharmonicity on the four lowest one-electron allowed photoionizations of SCl_2 in order to confirm and/or clarify assignments of the He I PE spectra reported in Refs. 8 and 9.

Since the two He I PE studies[8,9] appeared, some *ab initio* calculations on the $\tilde{X}\,^1A_1$ state of SCl_2 have been published.[11–14] However, the only *ab initio* investigation on SCl_2^+ is the modified coupled-pair functional (MCPF) calculations on the S 2*p* core-hole states of SCl_2^+.[15] There is no calculation available on any low-lying, valence cationic state of SCl_2^+ to our knowledge. On the experimental front, a large number of spectroscopic studies[16–28] have been carried out on SCl_2. For information on SCl_2^+, the only experimental studies are an x-ray PE and Auger study on the molecular field splitting in the S $2p_{3/2}$ core-ionization level of SCl_2^+,[15] the two He I PE studies[8,9] and the photoionization mass-spectrometry study[10] discussed above.

II. THEORETICAL CONSIDERATIONS AND COMPUTATIONAL DETAILS

A. *Ab initio* calculations

Geometry optimizations on the $\tilde{X}\,^1A_1$ state of SCl_2 and the $\tilde{X}\,^2B_1$, $\tilde{A}\,^2B_2$, $\tilde{B}\,^2A_1$, $\tilde{C}\,^2A_1$, $\tilde{D}\,^2A_2$, and $\tilde{E}\,^2B_2$ states of SCl_2^+ were carried out employing the restricted-spin coupled-cluster single and double plus perturbative triple excitation [RCCSD(T)] method.[29,30] Three different augmented-correlation-consistent-polarized basis sets of valence quadruple-zeta, valence quintuple-zeta, and core-valence quadruple-zeta quality, namely, the aug-cc-pV(Q+d)Z, aug-cc-pV(5+d)Z and aug-cc-pwCVQZ basis sets,[31,32] were used. With the first two valence basis sets, the frozen core

approximation was applied in the RCCSD(T) calculations. Effects of core electron correlation on computed minimum-energy geometries and relative electronic energies (AIEs and VIEs) were investigated using the aug-cc-pwCVQZ basis set, where only the S $1s^2$ and Cl $1s^2$ electrons were frozen in the RCCSD(T) calculations, i.e., the S $2s^22p^6$ and Cl $2s^22p^6$ electrons were included in the correlation calculations in addition to valence electrons.

Contributions of basis set extension to the complete basis set (CBS) limit to the computed AIE and VIE values were estimated[33] by taking half of the differences between the corresponding values obtained using the aug-cc-pV(5+*d*)Z and aug-cc-pV(Q+*d*)Z basis sets. Contributions of core electron correlation to the computed AIE and VIE values were estimated by taking the differences of the corresponding values obtained using the aug-cc-pwCVQZ basis set [including the S $2s^22p^6$ and Cl $2s^22p^6$ electrons in the RCCSD(T) calculations] and the aug-cc-pV(Q+*d*)Z basis set (within the frozen core approximation). The contributions of basis size extension and core electron correlation to the computed relative electronic energies have been assumed to be additive.

Relativistic effects, which include scalar (mass-velocity and Darwin terms) and spin-orbit contributions, for the second row elements, S and Cl, are not expected to be large. Nevertheless, scalar relativistic contributions to the computed AIE values have been computed explicitly by two different methods as implemented in the MOLPRO suite of programs.[34] First, the expectation values of the mass-velocity and Darwin terms were calculated employing the Cowan-Griffin operator with the Hartree-Fock wave function. Second, relativistic self-consisting field (SCF) calculations were carried out employing the Douglas-Kroll (DK) relativistic one-electron integrals. In this case, the relativistic contribution was taken as the difference between the total energies obtained from the relativistic DK calculation and the nonrelativistic Hartree-Fock calculation, $[E_{\mathrm{rel}}(\mathrm{DK})-E_{\mathrm{nonrel}}(\mathrm{HF})]$, employing the same basis set. The uncontracted *s*, *p*, and *d* primitive functions from the aug-cc-pV(Q+*d*)Z basis set were used in these relativistic calculations. Similar to the previous findings,[1,33] the results obtained employing the above-mentioned two methods are essentially identical and hence only one set of the results are presented below. It should also be noted that the uncontracted *s*, *p*, and *d* primitive functions from the cc-pV5Z-DK basis sets[35] for S and Cl, which were optimized for DK calculations, have also been employed to calculate relativistic contributions to AIEs as described above, and the results are essentially identical to those employing the uncontracted *s*, *p*, and *d* primitive functions of the aug-cc-pV(Q+*d*)Z basis sets. However, if the contracted form of the aug-cc-pVQZ basis sets or the cc-pV5Z-DK basis sets of S and Cl were used, the computed relativistic contributions obtained by using the Cowan-Griffin operator, and from the energy difference of $[E_{\mathrm{rel}}(\mathrm{DK})-E_{\mathrm{nonrel}}(\mathrm{HF})]$, differ significantly. This discrepancy arises from employing the same contracted basis sets, which were optimized for either HF or DF calculations, for both the HF and DK calculations. Nevertheless, when the uncontracted *s*, *p*, and *d* primitives of the basis sets optimized for either HF or DK calculations were used, they are shown to be flexible enough for both HF and DF calculations, and hence giving consistent results with both methods of calculating the relativistic contributions. Spin-orbit coupling effects have not been investigated, because all electronic states, neutral and cationic, considered have C_{2V} structures and hence are nondegenerate states, which do not have diagonal spin-orbit splitting. Off-diagonal spin-orbit interactions are only significant at regions where electronic energy surfaces of the states involved are close to each other, and they are expected to be weak for second row elements.

Some additional single geometry complete active space self-consisting field/multireference configuration interaction (CASSCF/MRCI) energy calculations[36,37] were carried out on the $\tilde{X}\,^1A_1$ state of SCl_2 and the two lowest doublet cationic states of each of the A_1, B_1, B_2, and A_2 symmetries of the C_{2V} point group. The aug-cc-pV(Q+*d*)Z basis set was used and the CASSCF/MRCI calculations were performed at the RCCSD(T) optimized geometry of the $\tilde{X}\,^1A_1$ state of SCl_2 using the same basis sets. A full valence active space was employed, and in the averaged-state CASSCF calculations, equal weights for the two lowest doublet states of each symmetry were used. These CASSCF/MRCI calculations give the VIEs to eight low-lying cationic states of SCl_2^+ and hence the relative electronic energies of these cationic states in the Franck-Condon (FC) region from the neutral ground state.

RCCSD(T) energy scans employing the aug-cc-pV(5+*d*)Z basis set were carried out on the $\tilde{X}\,^1A_1$ state of SCl_2 and the $\tilde{X}\,^2B_1$, $\tilde{A}\,^2B_2$, $\tilde{B}\,^2A_1$, $\tilde{C}\,^2A_1$, $\tilde{D}\,^2A_2$, and $\tilde{E}\,^2B_2$ states of SCl_2^+. The ranges of bond lengths and angles, and the number of energy points used in these energy scans are given in Table I. These energy points were used for the fitting of the potential energy function (PEF) of each electronic state considered (see Sec. III).

In addition to the computing vibrational frequencies by variational calculations to be described below, employing the RCCSD(T)/aug-cc-pV(5+*d*)Z PEFs just discussed, harmonic vibrational frequencies were also calculated numerically for the $\tilde{X}\,^1A_1$ state of SCl_2 and the $\tilde{X}\,^2B_1$ state of SCl_2^+ at their respective equilibrium geometries. These harmonic vibrational frequency calculations were carried out at the RCCSD(T) level with the aug-cc-pV(*Q*+*d*)Z basis set and they gave harmonic frequencies of all three vibrational modes (i.e., including the asymmetric stretching mode; variational calculations of anharmonic vibrational wave functions employing *ab initio* PEFs to be discussed have considered only the symmetric stretching and bending modes; see Sec. III). Zero-point energy correction (ΔZPE) for the first AIE of SCl_2 (i.e., the ionization leading to the $\tilde{X}\,^2B_1$ state of SCl_2^+) has been made using the computed harmonic vibrational frequencies of all three modes. ΔZPEs for higher AIEs, however, have been evaluated using only the computed fundamental frequencies of the symmetric stretching and bending modes obtained from the variational calculations using the *ab initio* PEFs. Based on computed vibrational frequencies of all three modes for the $\tilde{X}\,^1A_1$ state of SCl_2 and the $\tilde{X}\,^2B_1$ state of SCl_2^+, the difference between

including and excluding the asymmetric stretching mode in the evaluation of ΔZPE for the first AIE of SCl_2 is +0.0054 eV. In this connection, it seems reasonable to assume that the maximum uncertainties associated with the neglect of the asymmetric stretching mode in the evaluation of ΔZPE for higher IE bands are of the order of ±0.01 eV, and this has been included in the estimated uncertainties associated with the computed AIE_0 values of the higher IE bands.

All *ab initio* calculations in the present work were carried out using MOLPRO.[34]

III. POTENTIAL ENERGY FUNCTIONS, ANHARMONIC VIBRATIONAL WAVE FUNCTIONS, AND FRANCK-CONDON FACTOR CALCULATIONS

For each electronic state studied, the potential energy function (PEF), V, was determined by fitting the following polynomial to an appropriate number of single point energies obtained as discussed above:

$$V = \sum_{ij} C_{ij}(S_1)^i(S_2)^j + V_{\mathrm{eqm}} \tag{1}$$

S_1 (the symmetric stretching) in the PEF is expressed in terms of a Morse-type coordinate,[38]

$$S_1 = [1 - e^{-\gamma(r-r_{\mathrm{eqm}})/r_{\mathrm{eqm}}}]/\gamma, \tag{2}$$

where r is the SCl bond length and r_{eqm} is the equilibrium bond length. S_2 (the symmetric bending) is expressed as

$$S_2 = \Delta\theta + \alpha\Delta\theta^2 + \beta\Delta\theta^3, \tag{3}$$

where $\Delta\theta$ is the displacement in the θ(ClSCl) bond angle from the corresponding equilibrium value.[39] The nonlinear least squares fitting procedure,[40] NL2SOL, was employed to obtain the C_{ij}'s, V_{eqm}. r_{eqm}, θ_{eqm}, α, β, and γ values from the computed single point energy data. The asymmetric stretching mode has not been considered, because the observed first band in the He I PE spectrum of Ref. 9 with resolved vibrational structure does not show any identifiable vibrational structure associated with the asymmetric stretching mode, and for an ionization from a C_{2v} molecule to a C_{2v} cation, this mode is only allowed in double quanta excitations.

Variational calculations, which employed the rovibronic Hamiltonian of Watson for a nonlinear molecule[41] and the RCCSD(T)/aug-cc-pV(5+d)Z PEFs discussed above, were carried out to obtain the anharmonic vibrational wave functions and their corresponding energies (see Refs. 7 and 42 for details). The anharmonic vibrational wave functions were expressed as linear combinations of harmonic oscillator functions, $h(v_1,v_2)$, where v_1 and v_2 denote the quantum numbers of the harmonic basis functions for the symmetric stretching and bending modes, respectively.[7,42] The maximum v_1 and v_2 values of the harmonic basis used, and the restriction of the maximum magnitude of (v_1+v_2) imposed, for each electronic state studied are given in Table I. The FC factors were computed employing the anharmonic vibrational wavefunctions and allowing for the Duschinsky rotation, as described previously.[7,42]

Four PE bands, which lead to the $\tilde{X}\,^2B_1$, $\tilde{A}\,^2B_2$, $\tilde{C}\,^2A_1$, and $\tilde{D}\,^2A_2$ states of SCl_2^+ via one-electron allowed ionization processes, have been simulated. The relative intensity of each vibrational component in a simulated PE band is given by the corresponding computed anharmonic FC factor.

IV. RESULTS AND DISCUSSIONS

The coefficients of the fitted polynomials, C_{ij} [in Eq. (1)], the values of γ and α [in Eqs. (2) and (3), respectively], and the root-mean-square (rms) deviations of the fitted PEFs for the RCCSD(T)/aug-cc-pV(5+d)Z data points for the $\tilde{X}\,^1A_1$ state of SCl_2 and the $\tilde{X}\,^2B_1$, $\tilde{A}\,^2B_2$, $\tilde{C}\,^2A_1$, and $\tilde{D}\,^2A_2$ states of SCl_2^+ are given in Table II. *Ab initio* results obtained in the present study (equilibrium geometries, vibrational frequencies, AIEs and VIEs) are summarized in Tables III–VI together with available experimental and theoretical values for comparison. Simulated PE bands of SCl_2 are presented in Figs. 1–6.

A. The one-electron forbidden $\tilde{B}\,^2A_1$ and $\tilde{E}\,^2B_2$ states of SCl_2^+

The $\tilde{X}\,^1A_1$ state of SCl_2 has the electronic configuration $\cdots(11a_1)^2(4b_1)^2(8b_2)^2(2a_2)^2$. Following from our previous study on SF_2 and its low-lying cationic states,[1] in addition to the four cationic states of SCl_2^+ arising from ionizations of an electron from each of the highest doubly occupied molecular orbitals of each symmetry, we have also considered the one-electron forbidden $^2A_1$ and $^2B_2$ cationic states with the electronic configurations of $\cdots(12a_1)^1(3b_1)^2(8b_2)^2(2a_2)^2$ and $\cdots(11a_1)^2(3b_1)^2(9b_2)^1(2a_2)^2$, respectively. This is because in the case of SF_2^+, the corresponding one-electron forbidden cationic states, $(1)^2A_1$ and $(1)^2B_2$ states, are the $\tilde{A}\,^2A_1$ and $\tilde{B}\,^2B_2$ states, respectively, which lie below the one-electron allowed $\tilde{C}\,^2B_2$, $\tilde{D}\,^2A_1$ and $\tilde{E}\,^2A_2$ states. However, in the case of SCl_2^+, the order of the low-lying electronic states obtained here is $\tilde{X}\,^2B_1$, $\tilde{A}\,^2B_2$, $\tilde{B}\,^2A_1$, $\tilde{C}\,^2A_1$, $\tilde{D}\,^2A_2$, and $\tilde{E}\,^2B_2$ (see Tables III), which differs from that of SF_2^+ ($\tilde{X}\,^2B_1$, $\tilde{A}\,^2A_1$, $\tilde{B}\,^2B_2$, $\tilde{C}\,^2B_2$, $\tilde{D}\,^2A_1$, and $\tilde{E}\,^2A_2$).[1] For SCl_2^+, the one-electron forbidden cationic states are the $(1)^2A_1$ and $(2)^2B_2$ states, which are the $\tilde{B}\,^2A_1$ and $\tilde{E}\,^2B_2$ states (Table III).

Considering the two lowest $^2B_2$ states, the best computed AIE_0 (11.73 eV) and VIE_e (12.27 eV) of the one-electron allowed $\tilde{A}\,^2B_2$ state are lower than those of the one-electron forbidden $\tilde{E}\,^2B_2$ state (13.23 and 13.48 eV; see Table III) by 1.50 and 1.21 eV, respectively, indicating that the electronic energy surfaces of these two states are well separated in energy from each other in the region relevant to the PE spectrum of SCl_2. In addition, the computed CASSCF and MRCI wave functions of these two $^2B_2$ states of SCl_2^+ obtained from the two-state CASSCF/MRCI calculations at the minimum-energy geometry of the $\tilde{X}\,^1A_1$ state of SCl_2 show that there is negligible mixing between these two $^2B_2$ states through configuration interaction (CI) in the VIE region. Therefore, it is safely concluded that the one-electron forbidden ionization

TABLE II. RCCSD(T)/aug-cc-pV(5+*d*)Z potential energy functions (PEFs) of the $\tilde{X}\,^1A_1$ state of SCl_2 and the $\tilde{X}\,^2B_1$, $\tilde{A}\,^2B_2$, $\tilde{C}\,^2A_1$, and $\tilde{D}\,^2A_2$ states of SCl_2^+ (C_{ij}'s are the coefficients of the polynomials used for the PEFs [Eq. (1)]; see text).

C_{ij}	$\tilde{X}\,^1A_1$	$\tilde{X}\,^2B_1$	$\tilde{A}\,^2B_2$	$\tilde{C}\,^2A_1$	$\tilde{D}\,^2A_2$
C_{20}	2.926 956 0	3.514 468 0	2.971 042 9	2.580 540 0	2.607 750 6
C_{11}	0.122 355 8	0.165 276 7	0.511 859 2	0.243 015 0	0.119 068 7
C_{02}	0.125 268 0	0.142 0.51 4	0.214 404 5	0.077 604 8	0.111 562 1
C_{30}	−8.818 514 6	−6.372 016 0	−7.298 135 5	−8.761 068 7	−6.185 347 3
C_{21}	−0.741 182 0	−0.689 574 4	−2.000 323 5	−0.479 177 1	−0.747 722 8
C_{12}	−0.573 347 2	−0.586 310 5	−1.538 833 5	−0.242 627 6	−0.559 901 1
C_{03}	−0.031 856 9	0.005 046 5	−0.244 603 7	−0.012 180 7	0.008 244 8
C_{40}	15.94 778 8	4.603 394 1	9.228 616 9	20.29 869 2	8.183 861 2
C_{22}	1.300 714 5	0.812 739 6	1.807 628 4	1.008 026 5	1.447 169 6
C_{04}	0.082 098 4	0.075 698 1	0.396 376 5	0.012 406 5	0.079 592 0
C_{31}	0.316 844 6	0.112 903 2	0.545 040 8	−0.080 715 3	0.255 578 2
C_{13}	2.096 494 6	1.306 370 3	2.135 150 2	0.756 303 9	2.074 025 4
C_{05}	−0.040 811 2	0.048 879 6	−0.163 041 2	0.026 065 5	−0.104 008 3
C_{06}	0.098 729 8	0.164 018 9	−1.132 718 9	0.172 947 5	0.151 254 4
C_{50}	−24.54 293 8	−6.894 989 6	−9.346 981 8	−29.576 111	−9.903 276 8
C_{60}	35.139 972 0	−0.016 449 5	12.53 717 2	36.343 016	7.386 037 4
C_{41}	−2.347 208 7	−0.909 748 2	0.200 976 2	−0.099 924 1	−1.369 958 6
C_{32}	−0.830 572 9	−0.635 885 2	−0.076 260 6	−0.971 543 8	−0.523 967 4
C_{23}	−0.661 788 5	−1.013 660 3	−0.035 899 6	−0.638 415 4	−0.414 106 9
C_{14}	−0.495 128 5	−0.531 758 8	−0.372 517 1	−0.484 325 0	−0.723 954 2
C_{51}	0.047 725 8	0.062 287 1	1.637 687 2	0.180 943 1	0.437 641 2
C_{42}	−0.003 296 9	−0.027 089 1	2.350 580 2	0.062 585 4	0.194 814 7
C_{33}	−48.87 262 3	7.929 157 9	−13.483 627	−49.680 106	−4.411 639 4
C_{24}	41.541 785	7.287 261 9	−7.818 582 9	67.142 372	4.127 852 1
C_{15}	0.035 980 6	−3.067 566 9	1.036 723 1	44.377 851 2	−3.360 961 3
C_{07}	−1.281 041 9	−3.114 405 8	6.941 428 6	−1.662 930 6	−4.677 042 2
C_{08}	0.038 825 1	−2.130 385 3	9.319 861 7	−0.323 677 7	−1.589 308 5
C_{70}	0.295 298 2	−0.841 843 1	5.542 990 4	−0.519 455 0	−0.558 058 4
C_{80}	0.009 420 3	−0.144 943 7	0.600 882 6	−0.170 363 1	−0.596 702 4
α/rad^{-1}	0.202 646 8	1.455 134 8	0.775 603 7	0.135 170 9	0.866 435 0
γ	0.060 312 2	−0.022 923 4	0.102 900 4	−0.048 273 9	0.065 913 2
rms deviation/cm^{-1}	14.0	13.5	22.0	10.9	18.0

process to the $\tilde{E}\,^2B_2$ state of SCl_2^+ can be ignored in the consideration of the He I PE spectrum of SCl_2.

Considering the one-electron forbidden $\tilde{B}\,^2A_1$, state, the best computed VIE (13.27 eV; Table III) is higher than that of the one-electron allowed $\tilde{C}\,^2A_1$ state (12.51 eV) by 0.76 eV, suggesting that the electronic surfaces of these two states could interact via CI at the intersections. However, from the results of energy scans of the two $^2A_1$ states, the intersections between these two $^2A_1$ states are in the regions with θ of values around 130° and r of values larger than 2.2 Å, which are quite far away from the FC region of r =2.01 Å and θ=102.6° (the minimum of the $\tilde{X}\,^1A_1$ state of SCl_2; see Table IV), and also not near the minimum of the $\tilde{C}\,^2A_1$ ionic state (r_e=1.98 Å and θ_e=116.7°; see Table V). In addition, the one-electron forbidden $\tilde{B}\,^2A_1$ state of SCl_2^+, with a large minimum-energy bond angle of ca. 150° (see Table V), should have very poor FC factors with the $\tilde{X}\,^1A_1$ state of SCl_2, which has a computed θ_e of ca. 103° (Table V). This is reflected in the large difference of over 1.2 eV between the best computed AIE_0 and VIE_e for the ionization from the $\tilde{X}\,^1A_1$ state of SCl_2 to the $\tilde{B}\,^2A_1$ state of SCl_2 (Table III). Moreover, the computed CASSCF and MRCI wave functions of the $\tilde{B}\,^2A_1$ and $\tilde{C}\,^2A_1$ states of SCl_2^+ at the minimum-energy geometry of the $\tilde{X}\,^1A_1$ state of SCl_2 (i.e., at the VIE region) obtained in the two-state CASSCF/MRCI calculations show only very weak CI mixing between the two $^2A_1$ states. In addition, RCCSD(T) calculations on these two $^2A_1$ states at the VIE region give $T1$ diagnostic values of less than 0.029 for both states, suggesting negligible multireference character. Summing up, although the one-electron allowed $\tilde{C}\,^2A_1$ state could be perturbed by the one-electron forbidden $\tilde{B}\,^2A_1$ state near regions where the electronic surfaces of these two $^2A_1$ states cross each other, the above considerations suggest that such perturbation should be negligibly small near the FC region and hence would not be expected to affect the He I PE spectrum of SCl_2.

Summarizing, the optimized geometries, computed vibrational frequencies, and relative electronic energies of the one-electron forbidden $\tilde{B}\,^2A_1$ and $\tilde{E}\,^2B_2$ states of SCl_2^+ are included in the following subsections for the sake of completeness. However, in view of the above considerations, we

TABLE III. Computed adiabatic (AIE) and vertical (VIE) ionization energies (in eV) of some low-lying cationic states of SCl_2^+ obtained at different levels of calculation (see text).

	AIE		VIE	
State, open-shell conf.	RCCSD	RCCSD(T)	RCCSD	RCCSD(T)
$\tilde{X}\,^2B_1\ (4b_1)^1$				
Aug-cc-pV(Q+*d*)Z	9.551	9.527	9.740	9.688
Aug-cc-pV(5+*d*)Z	9.567	9.544	9.755	9.706
Aug-cc-pwCVQZ	9.557	9.530	9.751	9.693
(CBS+core)[a]		9.556±0.012		9.720±0.014
Relativistic[a]		−0.016±0.002		
Best AIE_e[a]		9.540±0.014		
Best AIE_0[a]		9.551±0.015		
He *I* photoelectron[b]		9.49		9.70
He *I* (second vibrational component)[b]		9.56[c]		
He *I* photoelectron[d]		9.47[c]		9.67
He *I* (second vibrational component)[d]		9.54[c]		
Photoionization mass spectrometry[e]		9.45(3)		
$\tilde{A}\,^2B_2\ (8b_2)^1$				
Aug-cc-pV(Q+*d*)Z	11.766	11.694	12.311	12.197
Aug-cc-pV(5+*d*)Z	11.792	11.722	12.343	12.231
Aug-cc-pwCVQZ	11.787	11.709	12.338	12.216
(CBS+core)		11.751±0.029		12.27±0.04
Relativistic		−0.028±0.003		
Best AIE_e		11.723±0.032		
Best AIE_0		11.73±0.04		
He *I* photoelectron[b]				12.24
He *I* photoelectron[d]				12.19 (a_1,b_2)
$\tilde{B}\,^2A_1\ (4b_1)^0(12a_1)^1$				
Aug-cc-pV(Q+*d*)Z	12.382	11.999	13.601	13.187
Aug-cc-pV(5+*d*)Z	12.413	12.035	13.638	13.227
Aug-cc-pwCVQZ	12.414	12.021	13.640	13.213
(CBS+core)		12.075±0.040		13.27±0.05
Relativistic		−0.035±0.004		
Best AIE_e		12.40±0.044		
Best AIE_0		12.03±0.05		
$\tilde{C}\,^2A_1\ (11a_1)^1$				
Aug-cc-pV(Q+*d*)Z	12.398	12.308	12.553	12.445
Aug-cc-pV(5+*d*)Z	12.424	12.338	12.583	12.477
Aug-c-pwCVQZ	12.421	12.327	12.580	12.465
(CBS+core)		12.372±0.034		12.51±0.04
Relativistic		−0.010±0.001		
Best AIE_e		12.362±0.035		
Best AIE_0		12.36±0.05		
He *I* photoelectron[b]				12.46 (a_1,a_2)
He *I* photoelectron[d]				12.19 (a_1,b_2)
$\tilde{D}\,^2A_2\ (2a_2)^1$				
Aug-cc-pV(Q+*d*)Z	12.776	12.547	12.852	12.625
Aug-cc-pV(5+*d*)Z	12.812	12.586	12.890	12.664
Aug-cc-pwCVQZ	12.815	12.572	12.891	12.651
(CBS+core)		12.631±0.045		12.71±0.05
Relativistic		−0.026±0.003		
Best AIE_e		12.605±0.048		
Best AIE_0		12.60±0.06		
He *I* photoelectron[b]				12.46 (a_1,a_2)
He *I* photoelectron[d]				12.45

TABLE III. (*Continued.*)

State, open-shell conf.	AIE		VIE	
	RCCSD	RCCSD(T)	RCCSD	RCCSD(T)
$\tilde{E}\,^2B_2$ $(4b_1)^0(9b_2)^1$				
Aug-cc-pV(Q+*d*)Z	13.584	13.175	13.763	13.403
Aug-cc-pV(5+*d*)Z	13.611	13.211	13.791	13.436
Aug-cc-pwCVQZ	13.622	13.204	13.801	13.429
(CBS+core)		13.258±0.047		13.48±0.04
Relativistic		−0.027±0.003		
Best AIE_e		13.231±0.050		
Best AIE_0		13.23±0.06		

[a]See text (same for below).
[b]Derived values using VIE values and vibrational separations given in Refs. 8 and 9; see text.
[c]Reference 8.
[d]Reference 9.
[e]Reference 10.

have neither calculated FC factors involving, nor simulated the ionization processes to, the two one-electron forbidden cationic states, for reasons given above.

B. Optimized geometrical parameters and computed vibrational frequencies

From Tables IV and V, the computed bond lengths, r_e(SCl), and bond angles, θ_e(ClSCl), obtained in the present study for the electronic states considered for SCl_2 and its cation, using the three basis sets described above, have the largest differences of <0.0083 Å and $<0.11°$, respectively, for a given state. The small ranges of these computed values show that a very high degree of consistency has been achieved in the computed minimum-energy geometrical parameters, particularly for bond angles. For computed bond lengths, both effects of basis set extension and core correlation lead to slightly smaller values, and core correlation effects are slightly larger in all cases. However, no general trend is observed for the computed bond angles from the results shown in Tables IV and V. For some electronic states, the core correlation and basis set extension effects on calculated bond angles reinforce each other, but for other states,

TABLE IV. Computed minimum-energy geometrical parameters (in angstrom and degree) and vibrational frequencies (foundamental frequencies in []; maximum uncertainties in (); cm^{-1}) of the $\tilde{X}\,^1A_1$ state of SCl_2 obtained at different levels of calculation from the present study (see text) and available calculated and experimental values.

$\tilde{X}\,^1A_1$	R(SCl)	θ(ClSCl)	ω_1	ω_2	ω_3	Reference
RCCSD(T)/AVQZ[a]	2.0197	102.62	528.3	206.4	529.1	Present
RCCSD(T)/AV5Z[b]	2.0160	102.59	535.1 [532.1]	209.3 [208.8]		Present
RCCSD(T)/ACVQZ[c]	2.0133	102.65				Present
Core+CBS	2.008(8)	102.61(2)				Present
MP2/6-311+G*	2.045	102.8				12
RCCSD(T)/CVQZ[d]	2.0142	102.71				13
Electron diffraction	1.99(3)	101(4)				24
Electron diffraction	2.00(2)	103(2)				25
Microwave r_0	2.014(2)	102.74				26
Microwave r_s	2.014(1)	102.64				26
Millimeter wave r_0	2.014(2)	102.74(18)				27
Millimeter wave r_s	2.0128(11)	102.71(9)				27
Raman liquid		100.03	[514(1)]	[208(1)]	[535(3)]	16
IR and Raman			[518.0]	[211]	[525.5]	18
IR gas			[525(15)]			17
Raman liquid			[514]	[208(3)]	535(15)	17
Raman			[528]	[205]	[525]	19
IR (Ne matrix)			[520]		[524]	20
IR (Ar matrix)				[208]		21
Raman liquid			[517]	[208]	[515]	23

[a]aug-cc-p(Q+*d*)Z.
[b]aug-cc-p(5+*d*)Z.
[c]aug-cc-pwCVQZ.
[d]cc-pCVQZ; see original work.

TABLE V. Computed minimum-energy geometrical parameters (in angstrom and degree) and vibrational frequencies (fundamental frequencies in []; maximum uncertainties in (); cm^{-1}) of some low-lying states of SCl_2^+ obtained at different levels of calculation (see text).

	R(SCl)	θ(ClSCl)	ω_1	ω_2	ω_3
$X\,^1B_1\ (4b_1)^1$					
RCCSD(T)/AVQZ	1.9362	106.82	592.6	234.3	616.0
RCCSD(T)/AV5Z	1.9330	106.80	598.2 [594.9]	238.1 [237.6]	
RCCSD(T)/ACVQZ	1.9298	106.87			
He *I* photoelectron[a]			[548]		
He *I* photoelectron[b]			[530(30)]		
$\tilde{A}\,^2B_2\ (8b_2)^1$					
RCCSD(T)/AVQZ	2.0486	78.24			
RCCSD(T)/AV5Z	2.0447	78.17	561.3 [558.3]	243.5 [241.5]	
RCCSD(T)/ACVQZ	2.0420	78.28			
$\tilde{B}\,^2A_1\ (12a_1)^1\ (4b_1)^0$					
RCCSD(T)/AVQZ	2.0261	149.03			
RCCSD(T)/AV5Z	2.0219	149.03	413.2 [414.4]	217.7 [208.6]	
RCCSD(T)/ACVQZ	2.0185	149.01			
$\tilde{C}\,^2A_1\ (11a_1)^1$					
RCCSD(T)/AVQZ	1.9894	116.65			
RCCSD(T)/AV5Z	1.9849	116.76	454.6 [452.1]	181.7 [181.0]	
RCCSD(T)/ACVQZ	1.9820	116.72			
$\tilde{D}\,^2A_2\ (2a_2)^1$					
RCCSD(T)/AVQZ	2.0709	95.87			
RCCSD(T)/AV5Z	2.0668	95.82	506.9 [503.8]	187.1 [186.4]	
RCCSD(T)/ACVQZ	2.0641	95.85			
$\tilde{E}\,^2B_2\ (4b_1)^0\ (9b_2)^1$					
Aug-cc-p-VQZ	2.0767	91.70			
Aug-cc-pV5Z	2.0710	91.74	780.2 [476.8]	266.2 [264.8]	
Aug-cc-pwCVQZ	2.0684	91.79			

[a]Reference 8.
[b]Reference 9.

they are in the opposite direction. Nevertheless, the spread of computed bond angles for all states studied are very small. There are no experimental geometrical parameters available for any cationic states of SCl_2^+ for comparison with our results. Therefore, the computed minimum-energy geometrical parameters shown in Table V are currently the most reliable for these states of SCl_2^+.

For the $\tilde{X}\,^1A_1$ state of SCl_2, some previous experimental and calculated geometrical parameters are available (Table IV). Particularly of note is a very recent computational study by Coriani *et al.*,[13] who have reported a very thorough investigation on the accuracy of *ab initio* molecular geometries for systems containing second row elements, which include SCl_2. In this study,[13] the HF, MP2, CCSD, and CCSD(T) levels of theory were considered and core correlation effects on geometrical parameters were investigated. However, the largest basis sets used were only up to quadruple-zeta quality, and diffuse functions (the augmented part of the correlation-consistent basis sets) have not been considered in Ref. 13. In the present study, we have employed augmented basis sets throughout, and also a basis set of quintuple quality. It seems clear that the calculations performed in the present study are currently of the highest level, and it was therefore decided not to include previous theoretical results in the following discussion.

The best theoretical values of r_e and θ_e obtained in the present study for the $\tilde{X}\,^1A_1$ state of SCl_2, assuming that core correlation and basis set extension effects on the computed geometrical parameters are additive (Core+CBS; Table IV), are 2.008 ± 0.008 Å and $102.61 \pm 0.02°$, respectively. The uncertainties quoted here are estimated from the differences between the best theoretical values and the calculated values obtained using the quintuple-zeta quality basis sets. The relatively large uncertainty of 0.008 Å associated with the computed bond length comes from the relatively large core correlation correction of −0.006 Å. The importance of core correlation effects on *ab initio* geometrical parameters for small molecules containing second row elements has been pointed out in Ref. 13.

The most reliable experimental geometrical parameters of the $\tilde{X}\,^1A_1$ state of SCl_2 currently available are the r_s geometrical parameters from the microwave study of Ref. 27. The best theoretical values reported here agree, within the estimated theoretical and/or experimental uncertainties, with

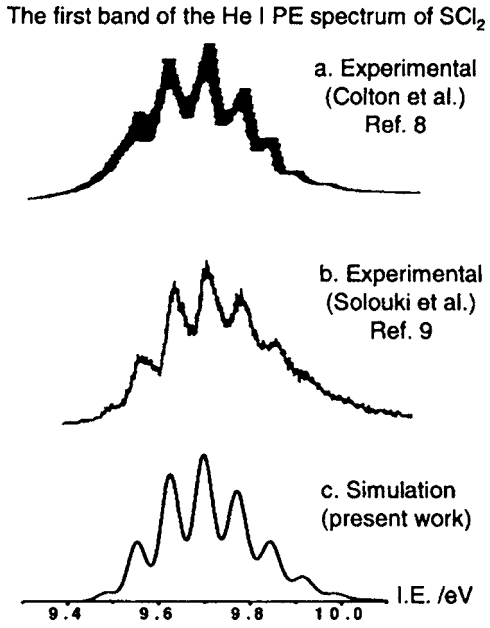

FIG. 1. The first band arising from the $SCl_2^+ \tilde{X}\,^2B_1 \leftarrow SCl_2\ \tilde{X}\,^1A_1$ ionization in the experimental He I photoelectron spectrum of SCl_2 from (a) Ref. 8 and (b) Ref. 9, and (c) the corresponding simulated spectrum employing the geometries of the $\tilde{X}\,^1A_1$ state of SCl_2 and the $\tilde{X}\,^2B_1$ states of SCl_2^+ obtained from the *ab initio* potential energy functions (see text), the best theoretical AIE_0 value (see Table III), a Boltzmann distribution of the low-lying vibrational levels of the $\tilde{X}\,^1A_1$ state of SCl_2 with a vibrational temperature of 300 K (see text) and a FWHM of 45 meV for each vibrational component.

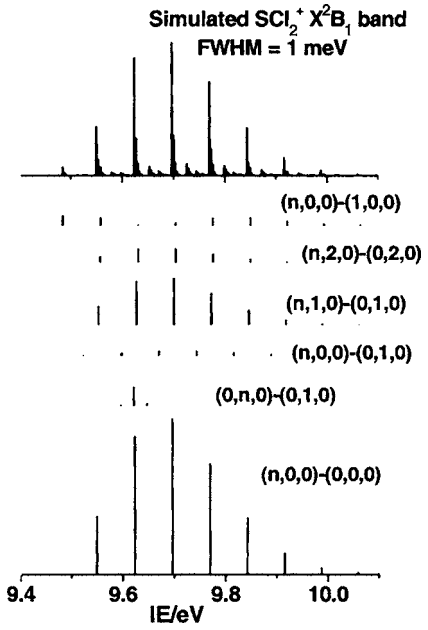

FIG. 2. The simulated first PE band arising from the $SCl_2^+ \tilde{X}\,^2B_1 \leftarrow SCl_2\ \tilde{X}\,^1A_1$ ionization with a FWHM of 1 meV [see also figure caption of Fig. 1(c)], and bar diagrams showing the computed FCFs and vibrational designations $[SCl_2^+ \tilde{X}\,^2B_1(\nu_1', \nu_2', \nu_3') \leftarrow SCl_2\ \tilde{X}\,^1A_1(\nu_1'', \nu_2'', \nu_3'')]$ of some major vibrational progressions contributing to the PE band.

the most reliable experimental r_s values of 2.0128±0.0011 Å; 102.71±0.09° of Ref. 27 (Table IV).

Considering vibrational frequencies, the only available experimental information for SCl_2^+ is from the He I PE spectra of Refs. 8 and 9, which give the symmetric stretching frequency, ν_1', of the $\tilde{X}\,^2B_1$ state of SCl_2^+ values of 548 and 530±30 cm^{-1}, respectively (Table V). The corresponding computed fundamental vibrational frequency obtained from the RCCSD(T)/aug-cc-pV(5+*d*) PEF in the present study is 594.9 cm^{-1}. The experimental values are smaller than the current best theoretical value from the present work by ca. 50 cm^{-1}. For the computed harmonic vibrational frequencies (both ω_1 and ω_2; see Table V) of the $\tilde{X}\,^2B_1$ state of SCl_2^+ obtained employing the aug-cc-pV(Q+*d*)Z (computed numerically) and aug-cc-pV(5+*d*)Z (computed variationally using the *ab initio* PEF) basis sets, the maximum differences in ω_1 or ω_2 are less than 6 cm^{-1}. The maximum uncertainty associated with the computed vibrational frequencies is therefore not expected to be larger than ca. 10 cm^{-1}. Both experimental He I PE studies of Refs. 8 and 9 have not given the resolution of their spectra explicitly. Nevertheless, comparing the simulated first PE band, which has employed a resolution of 45 meV (362 cm^{-1}) full width at half maximum (FWHM), with the experimental spectra of Refs. 8 and 9 (see Fig. 1), it is clear that the two experimental spectra have resolutions significantly poorer than 45 meV FWHM. It should also be noted that the energy scale of 8.3–9.1 eV in the expanded spectrum of the first PE band of SCl_2 given in Fig. 2 of Ref. 9 is clearly erroneous, as the VIE given for the first PE band of SCl_2 in the same publication is 9.67 eV, which is outside the energy scale of 8.3–9.1 eV given in their Fig. 2. In view of the above considerations, it is concluded that the uncertainty associated with the experimental symmetric stretching frequency of the $\tilde{X}\,^2B_1$ state of SCl_2^+ is probably larger than ±30 cm^{-1} given in Ref. 9 and the agreement between the computed υ_1' value of the $\tilde{X}\,^2B_1$ state of SCl_2^+ obtained here and the available experimental values reported in Refs. 8 and 9 may be considered to be just within the combined experimental and theoretical uncertainties. However, we note here that the reported experimental υ_1' ionic values[8,9] of 548 and 530 cm^{-1} (Table V) obtained from the first band in the He I PE spectra of SCl_2 are actually close to available υ_1'' neutral values of 510–530 cm^{-1} (Table IV). We will come back to this, when the simulated and observed first PE band of SCl_2 are compared.

For the $\tilde{X}\,^1A_1$ state of SCl_2, vibrational frequencies for all three vibrational modes obtained from a large number of Raman and infrared studies[16–23] are given in Table IV. It is pleasing that comparison between computed and available experimental values gives discrepancies between theory and experiment of less than 18 cm^{-1} (see Table IV).

C. Relative electronic energies: Vertical and adiabatic ionization energies

The best theoretical value of the first AIE_e of SCl_2 obtained in the present study, which includes contributions from core electron correlation, basis set extension (to the CBS limit) and relativistic effects is 9.540±0.014 eV (see Table III). Contributions from both core electron correlation and basis set extension increase the computed AIE_e value slightly, but the relativistic contribution decreases it slightly. The core correlation contribution is small (+0.003 eV), but

TABLE VI. Computed vertical (VIE*e*) ionization energies (in eV) of some low-lying cationic states of SCl_2^+ obtained at the CASSCF/MRCI and RCCSD(T) levels of calculation, using the aug-cc-pV(Q+d)Z basis set, at the RCCSD(T) minimum-energy geometry of the $\tilde{X}\,^1A_1$ state of SCl_2 using the same basis set.

State, Config.	MRCI	MR+D[a]	RCSD(T)	Best VIE_e[b]	He *I*[c]	He *I*[d]	*KT*[e]
$^1B_1$ $(4b_1)^1$	9.34	9.52	9.69	9.72	9.70	9.67	10.03
$^2B_2$ $(8b_2)^1$	11.94	12.07	12.20	12.27	12.24	12.19	12.75
$^2A_1$ $(11a_1)^1$	12.19	12.30	12.44	12.51	12.46	12.19	12.69
$^2A_2$ $(2a_2)^1$	12.34	12.45	12.63	12.71	12.46	12.45	13.41
$^2A_1$ $(12a_1)^1$ $(4b_1)^0$	12.94	13.03	13.19	13.27	[f]		
$^2B_2$ $(4b_1)^0$ $(9b_2)^1$	13.17	13.24	13.40	13.48	[f]		
$^2B_1$ $(3b_1)^1$ $(4b_1)^2$	13.78	13.89			14.05	13.91	15.37
$^2A_2$	14.47	14.55			[f]		
$(12a_1)^1$ $(4b_1)^1$ $(8b_2)^1$							
					14.75(b_2)	14.67(a_1)	

[a]MRCI plus Davidson corrections.
[b]Best VIE_e values from the present study (see Table III).
[c]Experimental values from Ref. 8.
[d]Experimental values from Ref. 9.
[e]Koopmans' theorem values from Ref. 9 (HF/[7*s*4*p*1*d*] calculations).
[f]These cationic states cannot be reached via one-electron ionization processes, and hence are formally forbidden; see text.

the relativistic contribution of −0.016 eV is larger than the basis set extension contribution of +0.009 eV. The maximum theoretical uncertainty associated with the best AIE_e value has been estimated based on the difference between the best AIE_e value and the calculated RCCSD(T) value using the valence quintruple-zeta quality basis set, plus an estimated uncertainty of 0.002 eV associated with the relativistic contribution (10% of the relativistic contribution). Including ΔZPE as discussed earlier, the first AIE_0 of SCl_2 has a best theoretical value of 9.551±0.015 eV (the quoted uncertainty has included an estimated uncertainty associated with ΔZPE of 0.001 eV, which is 10% of the ΔZPE value). Comparing the best theoretical AIE_0 value of SCl_2 obtained here with available experimental values of 9.49, 9.47, and 9.45±0.03 eV from Refs. 8–10, respectively, the discrepancies between theory and experiment are larger than 0.06 eV, which is larger than the combined theoretical and experimental uncertainties by ca. 0.03 eV. We just note here that the positions of the second vibrational component in the first PE band of the two He I PE spectra of SCl_2 can be evaluated using the vibrational spacings given in the two studies of Refs. 8 and 9, and they are 9.56 and 9.54 eV, respectively (see Table III). These estimated positions of the second vibrational component in the first band of the two He I PE studies agree, within the estimated theoretical uncertainty, with the best *ab initio* value of 9.551 eV obtained from the present study. We will come back to this in the subsection on FC simulations of the first PE band of SCl_2.

Regarding the computed AIE_e values for ionizations leading to the excited states of SCl_2^+ considered, contributions from both core correlation and basis set extension to the CBS limit are significantly larger in magnitude than those for the first AIE_e discussed. Consequently, larger uncertainties are associated with the computed AIE_0 (and also VIE_e) values to the excited cationic states considered than to the $\tilde{X}\,^2B_1$ state of SCl_2^+ (see Table III). Nevertheless, both core correlation and basis set extension contributions lead to a larger AIE_e value in all cases. At the same time, although the magnitudes of the computed relativistic contributions vary, depending on the particular cationic state, they decrease the computed AIE_e value in all cases.

For the higher IE bands of SCl_2 in the available observed He I PE spectra,[8,9] no AIE position is given, probably because no vibrational structure could be resolved in these PE bands. Nevertheless, their VIE positions are given, and assignments have been made based on computed VIEs as mentioned in the Introduction. Some of the computed and experimental VIE values from Refs. 8 and 9 are compared with the computed VIE values obtained here in Table VI (see also Table III). Firstly, it should be noted that the true VIE position of a PE band depends on the FC factors between the two states involved. Therefore, comparison between computed *ab initio* and observed VIE positions can only be useful as a guide to band assignment. Secondly, the best *ab initio* VIEs to the $\tilde{A}\,^2B_2$, $\tilde{C}\,^2A_1$, and $\tilde{D}\,^2A_2$ states of SCl_2^+ are within the IE region of 11.5–13.5 eV, covered by the observed second and third bands in the He I PE spectrum (see Fig. 2). The observed fourth PE band, with experimental VIE values of 14.05 and 13.92 eV from Refs. 8 and 9, respectively (see Table VI), is ca. 1.5 eV higher in energy than that of the observed third PE band. It is clear that the observed fourth PE band of SCl_2 cannot be assigned to the ionization to any of the $\tilde{A}\,^2B_2$, $\tilde{C}\,^2A_1$, and $\tilde{D}\,^2A_2$ states of SCl_2^+. Ionizations to these three cationic states have to be associated with the observed second and third PE bands. Thirdly, our best computed *ab initio* VIE values of 12.27 and 12.51 eV for the ionizations to the $\tilde{A}\,^2B_2$ and $\tilde{C}\,^2A_1$ states respectively agree very well with the experimental VIE values of 12.24 and 12.56 eV for the observed second and third PE bands of SCl_2 from Ref. 8 (see Table VI). In this connection, the observed second and third bands in the experimental PE spectrum can be assigned to ionization to the $\tilde{A}\,^2B_2$ and $\tilde{C}\,^2A_1$ states, respectively. These assignments support those given in Ref. 8.

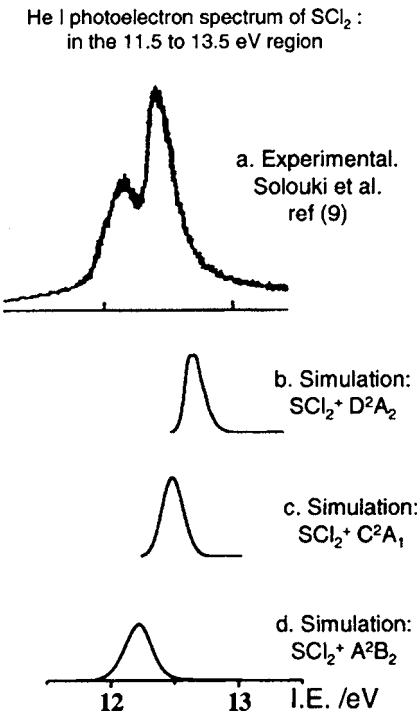

FIG. 3. (a) The experimental He I photoelectron spectrum of SCl_2 in the 11.5–13.5 eV region (from Ref. 9; see text), and the simulated ionizations from the $\tilde{X}\,^1A_1$ state of SCl_2 to the $\tilde{D}\,^2A_2$ (b), $\tilde{C}\,^2A_1$ (c), and $\tilde{A}\,^2B_2$ (d) states of SCl_2^+; a FWHM of 45 meV for each vibrational component has been used in the simulated spectra (see Figs. 4–6, and also text for details)

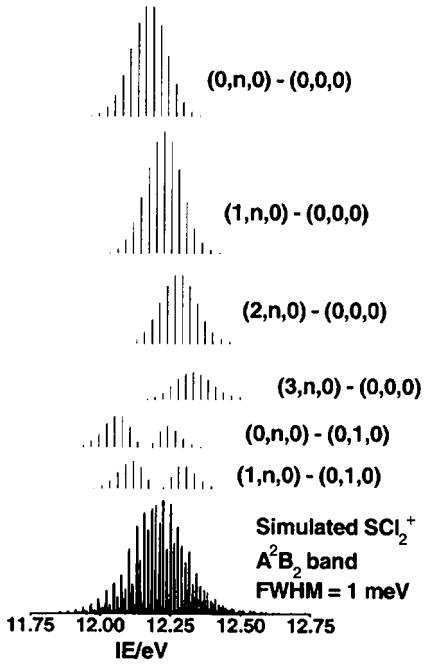

FIG. 4. The simulated spectrum of the $SCl_2^+\ \tilde{A}\,^2B_2 \leftarrow SCl_2\ \tilde{X}\,^1A_1$ ionization, employing the corresponding geometries obtained from the *ab initio* potential energy functions (see text), the best theoretical AIE_0 value (see Table III), a Boltzmann distribution for the low-lying vibrational levels of the $\tilde{X}\,^1A_1$ state of SCl_2 with a vibrational temperature of 300 K (see text) and a FWHM of 1 meV for each vibrational component (see text); the bar diagrams show the computed FCFs and vibrational designations $[SCl_2^+\ \tilde{A}\,^2B_2(\nu_1',\nu_2',\nu_3') \leftarrow SCl_2\ \tilde{X}\,^1A_1(\nu_1'',\nu_2'',\nu_3'')]$ of some major vibrational progressions contributing to the PE band.

Considering ionization to the $\tilde{D}\,^2A_2$ state, the best *ab initio* VIE of 12.71 eV is higher in energy than the experimental VIE positions of the observed third PE band of 12.46 and 12.45 eV, given by Refs. 8 and 9, respectively, by ca. 0.24 eV. As mentioned above, FC factors may cause the observed VIE position to be different from the computed *ab initio* VIE position. Nevertheless, since the ionization to the $\tilde{D}\,^2A_2$ state cannot be associated with the fourth PE band, which is much higher in energy, it has to be associated with the observed third PE band. The assignment of the observed second and third PE bands will be further considered in the subsection on spectral simulations of the higher IE bands. Finally, our computed VIE to the $(2)^2B_1$ state of 13.89 eV at the CASSCF/MRCI+D level supports the assignment of the fourth PE band to this cationic state as given in Refs. 8 and 9 (see Table VI).

D. Spectral simulations: First PE band of SCl_2

The observed first band in the He I PE spectra of SCl_2 of Refs. 8 and 9, and the corresponding simulated spectrum obtained in the present investigation are compared in Fig. 1. In the spectral simulation, the geometries, as obtained from the respective *ab initio* PEFs of the two states involved, and the best theoretical AIE_0 value of 9.55 eV (Table V) were employed. A Boltzmann distribution with a vibrational temperature of 300 K has been assumed for the populations of the low-lying vibrational levels of the $\tilde{X}\,^1A_1$ state of SCl_2. A Gaussian function with a FWHM of 45 meV has been used for each vibrational component in Fig. 1. As mentioned above, the published experimental spectra [8,9] have a poorer resolution than 45 meV FWHM used in the simulated spectrum. In Fig. 2, the simulated first PE band of SCl_2 is given with a resolution of 1 meV FWHM in order to show contributions from weak vibrational progressions. The computed FC factors of the major vibrational progressions involved, including those of hot bands arising from ionizations from vibrationally excited levels of the $\tilde{X}\,^1A_1$ state of SCl_2, with their vibrational designations, are also shown as bar diagrams in Fig. 2.

First of all, it is pleasing to see that the simulated first PE band of SCl_2 obtained here matches very well with the corresponding observed spectra from Refs. 8 and 9 (Fig. 1). This confirms the molecular carrier of, and the electronic states involved in, the first band of the observed He I spectra to be SCl_2, and the $\tilde{X}\,^1A_1$ of SCl_2 and $\tilde{X}\,^2B_1$ state of SCl_2^+. In addition, it is concluded that the computed *ab initio* geometry change upon ionization is close to the true one, and the assumption of a Boltzmann distribution with a vibrational temperature of 300 K for the populations of low-lying vibrational levels of the $\tilde{X}\,^1A_1$ state of SCl_2 is reasonably valid.

Secondly, according to our computed FC factors and simulated spectra (Fig. 2), the first observable vibrational component in the first PE band of SCl_2 is a hot band corresponding to the ionization process of $SCl_2^+\ \tilde{X}\,^2B_1(0,0,0) \leftarrow SCl_2\ \tilde{X}\,^1A_1(1,0,0)$. Using the best *ab initio* AIE_0 value of 9.55 eV in the simulation, the position of this hot band vibrational component is 9.48 eV, in excellent agreement with the AIE position of 9.49 eV given in Ref. 8, and the derived

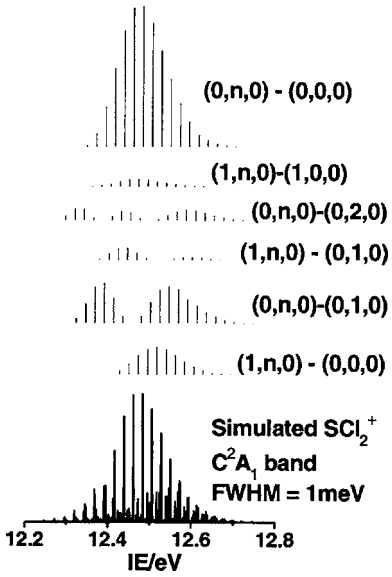

FIG. 5. The simulated spectrum of the $SCl_2^+ \tilde{C}\,^2A_1 \leftarrow SCl_2\ \tilde{X}\,^1A_1$ ionization, employing the corresponding geometries obtained from the *ab initio* potential energy functions (see text), the best theoretical AIE_0 value (see Table III), a Boltzmann distribution for the low-lying vibrational levels of the $\tilde{X}\,^1A_1$ state of SCl_2 with a vibrational temperature of 300 K (see text) and a FWHM of 1 meV for each vibrational component (see text); the bar diagrams show the computed FCFs and vibrational designations $[SCl_2^+ \tilde{C}\,^2A_1(\nu_1', \nu_2', \nu_3') \leftarrow SCl_2\ \tilde{X}\,^1A_1(\nu_1'', \nu_2'', \nu_3'')]$ of the major vibrational progressions contributing to the PE band.

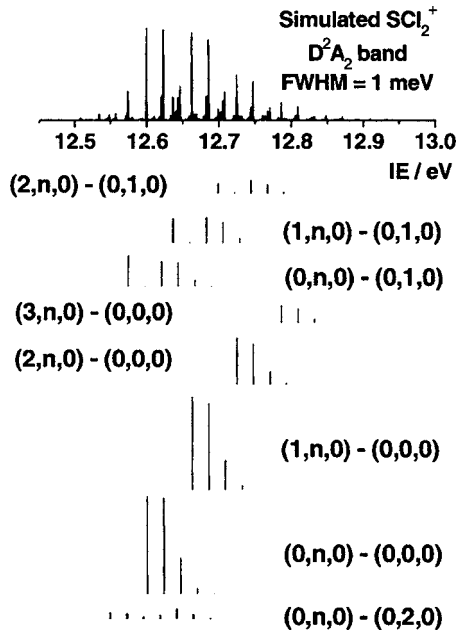

FIG. 6. The simulated spectrum of the $SCl_2^+ \tilde{D}\,^2A_2 \leftarrow SCl_2\ \tilde{X}\,^1A_1$ ionization, employing the corresponding geometries obtained from the *ab initio* potential energy functions (see text), the best theoretical AIE_0 value (see Table III), a Boltzmann distribution for the low-lying vibrational levels of the $\tilde{X}\,^1A_1$ state of SCl_2 with a vibrational temperature of 300 K (see text) and a FWHM of 5 meV for each vibrational component (see text); the bar diagrams show the computed FCFs and vibrational designations $[SCl_2^+ \tilde{D}\,^2A_2(\nu_1', \nu_2', \nu_3') \leftarrow SCl_2\ \tilde{X}\,^1A_1(\nu_1'', \nu_2'', \nu_3'')]$ of some major vibrational progressions contributing to the PE band.

AIE position of 9.47 eV from Ref. 9 (using the given VIE position and vibrational separations as described in the Introduction). The best *ab initio* AIE_0 value of 9.551 ± 0.015 eV also agrees very well with the experimental positions of the second vibrational component of the first PE band of SCl_2 of 9.56 and 9.54 eV derived from Refs. 8 and 9 as mentioned above. Summing up, the most important conclusion from the FC calculations performed in the present study is the revision of the experimental AIE_0 position of the first band in the He I PE spectra of SCl_2 from Refs. 8 and 9 to 9.55 ± 0.01 eV (the average of two experimental values). The excellent agreement between this revised experimental AIE_0 value and the best *ab initio* value also shows that the accuracy of an AIE obtained from state-of-the-art *ab initio* calculations, as carried out in the present investigation, is as high as ±0.01 eV, similar in magnitude to the theoretical uncertainty of ±0.015 eV estimated in this work.

Thirdly, based on the above revision of the vibrational assignment for the first PE band of SCl_2, the vibrational separation between the first identifiable vibrational component, i.e., the hot band, $SCl_2^+ \tilde{X}\,^2B_1(0,0,0) \leftarrow SCl_2\ \tilde{X}\,^1A_1(1,0,0)$ component, and the second vibrational component, i.e., the $\tilde{X}\,^2B_1(0,0,0) \leftarrow SCl_2\ \tilde{X}\,^1A_1(0,0,0)$ component corresponds actually to the vibrational separation in the υ_1'' mode of the neutral molecule, and not that of the υ_1' mode of the cation as assumed in Refs. 8 and 9. It appears that the wrong assignment of the hot band component to the $SCl_2^+ \tilde{X}\,^2B_1(0,0,0) \leftarrow SCl_2\ \tilde{X}\,^1A_1(0,0,0)$ component has led to smaller experimental vibrational separations of 548 and 530 cm^{-1} being given for the υ_1' frequency in Refs. 8 and 9, respectively, than the computed *ab initio* υ_1' value of 594.9 cm^{-1} obtained from the present study (see Table V). In this connection, the computed *ab initio* υ_1' value of 594.9 cm^{-1} obtained here is very likely more reliable than the experimental values given in Refs. 8 and 9.

E. Spectral simulations: Higher IE bands of SCl_2

The simulations of the PE bands corresponding to ionizations to the one-electron allowed $\tilde{A}\,^2B_2$, $\tilde{C}\,^2A_1$, and $\tilde{D}\,^2A_2$ states of SCl_2^+ from the $\tilde{X}\,^1A_1$ state of SCl_2 are given in Fig. 3, and compared with the observed second and third PE bands of Ref. 9, which gives a slightly cleaner spectrum of SCl_2 than Ref. 8. A resolution of 45 meV FWHM has been used for the simulated PE bands in Fig. 3. As can be seen from the simulated spectra in Fig. 3, with a resolution of 45 meV FWHM, no vibrational structure can be resolved in all three simulated bands. This is because the major vibrational progressions in these bands involve the bending mode with computed vibrational frequencies in the ranges of ca. 200 cm^{-1} (ca. 24 meV; see Table V and also Figs. 4–6). The simulated PE bands of these three one-electron allowed ionizations are, however, also presented individually in Figs. 4–6 with a resolution of 1 meV FWHM, in order to show their complex vibrational structures. Computed FC factors of the major vibrational progressions for ionizations to the $\tilde{A}\,^2B_2$, $\tilde{C}\,^2A_1$, and $\tilde{D}\,^2A_2$ states are also shown in Figs. 4–6, respectively, as bar diagrams together with their designations. Similar to the simulation of the first PE band of SCl_2 discussed above, *ab initio* geometries from the PEFs, the best *ab initio* AIE_0 values and a Boltzmann distribution with a

vibrational temperature of 300 K have been used in the simulation of these higher IE bands.

Firstly, from Fig. 3, comparison between simulated and observed spectra suggests the assignment of the $SCl_2^+ \tilde{A}\,^2B_2 \leftarrow SCl_2\ \tilde{X}\,^1A_1$ ionization to the observed second PE band (with the experimental VIEs of 12.24 and 12.19 eV from Refs. 8 and 9, respectively) and the assignment of the third PE band to contributions from both the ionizations to the $\tilde{C}\,^2A_1$ and $\tilde{D}\,^2A_2$ states of SCl_2^+ (with the experimental VIEs of 12.46 and 12.45 eV; see Table VI). It appears that, while the central part of the observed third PE band is due to ionization to the $\tilde{C}\,^2A_1$ state, the shoulder on the high IE side of the observed third PE band is due to ionization to the $\tilde{D}\,^2A_2$ state. In summary, based on the FC simulations of the present study, the assignments of Ref. 8 for the second and third PE bands of SCl_2 is preferred to those of Ref. 9.

Considering the vibrational structure associated with the ionization process of $SCl_2^+ \tilde{A}\,^2B_2 \leftarrow SCl_2\ \tilde{X}\,^1A_1$, it can be seen from Fig. 4 that the main vibrational progressions involved are $(1,v_2',0) \leftarrow (0,0,0)$, $(0,v_2',0) \leftarrow (0,0,0)$, and $(2,v_2',0) \leftarrow (0,0,0)$. Hot bands series, $(0,v_2',0) \leftarrow (0,1,0)$ and $(1,v_2',0) \leftarrow (0,1,0)$, also have significant contributions. From the computed FC factors, the $(0,0,0) \leftarrow (0,0,0)$ vibrational component at 11.73 eV (i.e., the AIE_0 position; Table III) is too weak to be observed in the simulated spectrum (see Fig. 4) and the first identifiable vibrational component in the strongest main series of $(1,v_2',0) \leftarrow (0,0,0)$ is with $v_2'=7$. The strongest vibrational component in the simulated band to the $\tilde{A}\,^2B_2$ state is $(1,15,0) \leftarrow (0,0,0)$ at 12.22 eV (i.e., the VIE position). The large change in the equilibrium bond angle upon ionization from ca. 102 to 78° (Tables IV and V) leads to ionizations to highly excited vibrational levels in the bending mode of the upper cationic state.

For the $\tilde{C}\,^2A_1$ PE band, the major vibrational progression is $(0,v_2',0) \leftarrow (0,0,0)$ (see Fig. 5). However, the $(1,v_2',0) \leftarrow (0,0,0)$ progression, and the hot band series, $(0,v_2',0) \leftarrow (0,1,0)$ and $(0,v_2',0) \leftarrow (0,2,0)$, also have significant contributions. The strongest vibrational components in the major series of $(0,v_2',0) \leftarrow (0,0,0)$ are with $v_2'=6$ and 5, at IEs of 12.51 and 12.44 eV, respectively. Consequently, the VIE position derived from FC simulation is at ca. 12.48 eV, in reasonably good agreement with the experimental values of 12.46 and 12.45 eV from Refs. 8 and 9, respectively. It can been seen from Fig. 5 that, the $(0,0,0) \leftarrow (0,0,0)$ vibrational component is weak, and also there are hot bands with significant relative intensities to the low IE side of the $(0,0,0) \leftarrow (0,0,0)$ component. Consequently, it is not possible to identify the AIE_0 position from comparison between the simulated and observed spectra, unless much better resolved PE spectra than those of Refs. 8 and 9 are available. Nevertheless, the very good agreement between the experimental and theoretical (from *ab initio* calculations and FC simulations) VIE values suggests that the best *ab initio* AIE_0 used in the spectral simulation is probably reliable.

For the $\tilde{D}\,^2A_2$ PE band, the two main vibrational progressions are $(0,v_2',0) \leftarrow (0,0,0)$ and $(1,v_2',0) \leftarrow (0,0,0)$ (see Fig. 6). The $(2,v_2',0) \leftarrow (0,0,0)$ progression and a number of hot band series also contribute, as shown in Fig. 6. It is interesting to note that the strongest vibrational component in the simulated band is, in fact, $(0,0,0) \leftarrow (0,0,0)$ at the AIE_0 position of 12.60 eV (Table III). In addition, the $(0,1,0) \leftarrow (0,0,0)$, $(1,0,0) \leftarrow (0,0,0)$, and $(1,1,0) \leftarrow (0,0,0)$ components are also very strong. Consequently, the overall computed FC envelope has an asymmetric shape with a relatively sharp rise on the low IE side and a gradually descending slope on the high IE side (see Figs. 3 and 6). Without the hot bands, the rise on the low IE side of the $\tilde{D}\,^2A_2$ PE band will be even sharper. Summing up, the computed FC envelope suggests a lower VIE position, which is near the AIE region (at ca 12.60 eV), than the *ab initio* suggested VIE (12.71 eV; Table VI). In addition, the simulated overall band shape suggests that the shoulder at the higher IE side of the observed third PE band of SCl_2 is mainly due to ionization to the $\tilde{D}\,^2A_2$ state.

V. CONCLUDING REMARKS

We have carried out extensive *ab initio* calculations on SCl_2 and some low-lying cationic states of SCl_2^+. Employing RCCSD(T)/aug-cc-pV(5+*d*)Z potential energy functions, we have calculated anharmonic vibrational wave functions of all these neutral and cationic states and also FC factors including the Duschinsky rotation and anharmonicity for ionizations from the $\tilde{X}\,^1A_1$ state of SCl_2 to the one electron allowed $\tilde{X}\,^2B_1$, $\tilde{A}\,^2B_2$, $\tilde{C}\,^2A_1$, and $\tilde{D}\,^2A_2$ states of SCl_2^+. Comparison between the simulated PE spectrum of the $SCl_2^+ \tilde{X}\,^2B_1 \leftarrow SCl_2\ \tilde{X}\,^1A_1$ ionization, obtained using computed FC factors from the present study, with the first band in the available experimental He I PE spectra[8,9] of SCl_2 leads to the revision of the first AIE_0 value of SCl_2 to 9.55 ± 0.01 eV. This revision is based on our FC spectral simulations, which show that the observed first vibrational component in the first PE band is a vibrational hot band: $SCl_2^+ \tilde{X}\,^2B_1(0,0,0) \leftarrow SCl_2\ \tilde{X}\,^1A_1(1,0,0)$. In this connection, the reliability of the experimental v_1' vibrational frequencies reported previously[8,9] for the $\tilde{X}\,^2B_1$ state of SCl_2^+, which were obtained based on the erroneous assignment of the first vibrational component in the first PE band to the $SCl_2^+ \tilde{X}\,^2B_1(0,0,0) \leftarrow SCl_2\ \tilde{X}\,^1A_1(0,0,0)$ vibrational component, is in doubt. Further experimental investigation is required to obtain a reliable experimental value of v_1' for the $\tilde{X}\,^2B_1$ state of SCl_2^+. It is concluded that the computed v_1' vibrational frequency obtained in the present work is currently the most reliable.

Simulated higher IE bands of SCl_2 have been compared with available experimental He I spectra[8,9] and support the assignments of the $SCl_2^+ \tilde{A}\,^2B_2 \leftarrow SCl_2\ \tilde{X}\,^1A_1$ ionization to the observed second band, and the ionizations to the $\tilde{C}\,^2A_1$ and $\tilde{D}\,^2A_2$ states of SCl_2^+ to the observed third band in the experimental He I PE spectra.[8,9] The computed FC envelopes of the latter two ionizations to the $\tilde{C}\,^2A_1$ and $\tilde{D}\,^2A_2$ states suggest that the ionization to the $\tilde{C}\,^2A_1$ state contributes mainly to the central part of the observed third PE band, while the ioniza-

tion to the $\tilde{D}\,^2A_2$ state with a simulated asymmetric band shape contributes mainly to the high IE shoulder of the observed third PE band.

It is noted that we have not applied the iterative Franck-Condon analysis[42,43] (IFCA), where geometry changes upon ionization are varied systematically over a small range until the best match between the simulated and observed spectra is obtained, in the present study. We have also not varied the vibrational temperature used for the Boltzmann distribution of vibrational population in the low-lying levels of the $\tilde{X}\,^1A_1$ state of SCl_2 in order to obtain a better match between the simulated and observed spectra. For the higher IE bands in the available He I experimental spectra[8,9] of SCl_2, where no resolvable vibrational structure has been observed, comparison between simulated and observed PE bands can only be qualitative. It is, therefore, not very meaningful to try to achieve a better match between the simulated and observed spectra than what has already been achieved. Nevertheless, assuming that the *ab initio* geometries and relative electronic energies used in the simulation are reliable, spectral simulations from the present study marginally savour the slightly higher VIE values of 12.24 and 12.46 eV of Ref. 8 to the slightly lower VIE values of 12.19 and 12.45 eV of Ref. 9, for the second and third PE bands of SCl_2, respectively.

For the first PE band of SCl_2, resolvable vibrational structure was observed in both He I spectra of Refs. 8 and 9. However, the experimental resolution in these references appears to be significantly poorer than 45 meV FWHM used in the spectral simulations. Nevertheless, the agreement between the "purely theoretical" and observed spectra as shown here is already very good. This implies that the *ab initio* calculations carried out in the present investigation are highly reliable. In conclusion, we have reported highly reliable simulated PE bands of SCl_2, based on combined high-level *ab initio* and FC calculations which include anharmonicity, and have made significant contributions to the assignments of available He I PE spectra of SCl_2. Finally, it is concluded that state-of-the-art *ab initio* calculations, such as those performed in the present study, are able to give computed AIEs to within an accuracy of up to ±0.01 eV for a triatomic molecule containing second row elements.

ACKNOWLEDGMENTS

Financial support from the Research Grant Council (RGC) of the Hong Kong Special Administrative Region (HKSAR, Grant Nos. AoE/B-10/1 PolyU and PolyU 5003/04P) and provision of computational resources from the EPSRC (UK) National Service for Computational Chemistry Software are acknowledged.

[1] E. P. F. Lee, D. K. W. Mok, F.-T. Chau, and J. M. Dyke, J. Chem. Phys. **125**, 104304 (2006), following paper.
[2] M. de Leeuw, R. Mooyman, and C. A. de Lange, Chem. Phys. **34**, 287 (1978).
[3] F.-T. Chau, D. K. W. Mok, E. P. F. Lee, and J. M. Dyke, ChemPhysChem **6**, 2037 (2005).
[4] J. M. Dyke, E. P. F. Lee, D. K. W. Mok, and F.-T. Chau, ChemPhysChem **6**, 2046 (2005).
[5] E. P. F. Lee, D. K. W. Mok, F.-T. Chau, and J. M. Dyke, J. Chem. Phys. **121**, 2962 (2004).
[6] E. P. F. Lee, D. K. W. Mok, J. M. Dyke, and F.-T. Chau, J. Chem. Phys. **106**, 10130 (2002).
[7] D. W. K. Mok, E. P. F. Lee, F.-T. Chau, D.-C. Wang, and J. M. Dyke, J. Chem. Phys. **113**, 5791 (2000).
[8] R. J. Colton and J. W. Rabalais, J. Electron Spectrosc. Relat. Phenom. **3**, 345 (1974).
[9] B. Solouki, P. Rosmus, and H. Bock, Chem. Phys. Lett. **26**, 20 (1974).
[10] R. Kaufel, G. Vahl, R. Minkwitz, and H. Baumgartel, Zeit. Fur Anorgan. Und Allgem. Chem. **481**, 207 (1981).
[11] G. L. Gutsev, J. Phys. Chem. **96**, 10242 (1992).
[12] Y. Drozdova, R. Steudel, W. Koch, K. Miaskiewicz, and I. A. Topol, Chem.-Eur. J. **5**, 1936 (1999).
[13] S. Coriani, D. Marchesan, J. Gauss, C. Hattig, T. Helgaker, and P. Jorgensen, J. Chem. Phys. **123**, 184107 (2005).
[14] J. H. Wang and V. H. Smith, Z. Naturforsch., A: Phys. Sci. **48**, 699 (1993).
[15] K. J. Borve, L. J. Saethre, and S. Svensson, Chem. Phys. Lett. **310**, 439 (1999).
[16] H. Stammreich, R. Forneris, and K. Sone, J. Chem. Phys. **23**, 972 (1955).
[17] T. Shimanouchi, J. Phys. Chem. Ref. Data **6**, 993 (1972).
[18] R. Sovie and J. Tremblay, Can. J. Spectrosc. **17**, 73 (1972).
[19] S. G. Frankiss and D. J. Harrison, Spectrochim. Acta, Part A **31**, 161 (1975).
[20] D. Bielefeldt and H. Willner, Spectrochim. Acta, Part A **36**, 989 (1980).
[21] M. Feuerhahn and G. Vahl, Inorg. Nucl. Chem. Lett. **16**, 5 (1980).
[22] R. Minkwitz, U. Nass, and J. Sawatzki, J. Fluorine Chem. **31**, 175 (1986).
[23] R. Steudel, D. Jensen, and B. Plinke, Z. Naturforsch. B **42**, 163 (1987).
[24] K. J. Palmer, J. Am. Chem. Soc. **60**, 2360 (1938).
[25] D. P. Stevenson and I. Y. Beach, J. Am. Chem. Soc. **60**, 2872 (1938).
[26] R. W. Davis and M. C. L. Gerry, J. Mol. Spectrosc. **65**, 455 (1977).
[27] L. Bizzocchi, L. Cludi, C. D. Esposti, and A. Giorgi, J. Mol. Spectrosc. **204**, 275 (2000).
[28] K. Gholivand and A. Eskami, Phosphorus, Sulfur Silicon Relat. Elem. **116**, 269 (1996).
[29] C. Hampel, K. Peterson, and H.-J. Werner, Chem. Phys. Lett. **190**, 1 (1992).
[30] J. D. Watts, J. Gauss, and R. J. Bartlett, J. Chem. Phys. **98**, 8718 (1993).
[31] T. H. Dunning, Jr., K. A. Peterson, and A. K. Wilson, J. Chem. Phys. **114**, 9244 (2001).
[32] K. A. Peterson and T. H. Dunning, J. Chem. Phys. **117**, 10548 (2002).
[33] E. P. F. Lee, J. M. Dyke, F.-T. Chau, and W.-K. Chow, Chem. Phys. Lett. **376**, 465 (2003).
[34] H.-J. Werner, P. J. Knowles, R. D. Amos *et al.*, MOLPRO, a package of *ab initio* programs version 2002.1.
[35] A. K. Wilson, D. E. Woon, K. A. Peterson, and T. H. Dunning, Jr., J. Chem. Phys. **110**, 7667 (1999).
[36] H.-J. Werner and P. J. Knowles, J. Chem. Phys. **82**, 5053 (1985).
[37] P. J. Knowles and H.-J. Werner, Chem. Phys. Lett. **145**, 514 (1988).
[38] W. Meyer, P. Botschwina, and P. Burton, J. Chem. Phys. **84**, 891 (1986).
[39] S. Carter and N. C. Handy, J. Chem. Phys. **87**, 4294 (1987).
[40] J. E. Dennis, Jr., D. M. Gay, and R. E. Welsh, ACM Trans. Math. Softw. **7**, 348 (1981).
[41] J. K. G. Watson, Mol. Phys. **19**, 465 (1970).
[42] F.-T. Chau, J. M. Dyke, E. P. F. Lee, and D. K. W. Mok, J. Chem. Phys. **115**, 5816 (2001).
[43] F. T. Chau, J. M. Dyke, E. P. F. Lee, and D. K. W. Mok, J. Chem. Phys. **118**, 4025 (2003).